

© 2017 IEEE. Personal use of this material is permitted. Permission from IEEE must be obtained for all other uses, in any current or future media, including reprinting/republishing this material for advertising or promotional purposes, creating new collective works, for resale or redistribution to servers or lists, or reuse of any copyrighted component of this work in other works.

Passive Forward Scatter Radar based on satellite TV broadcast for air target detection: preliminary experimental results

Andrea Arcangeli, Carlo Bongioanni, Nertjana Ustalli, Debora Pastina, Pierfrancesco Lombardo

DIET Dept., Sapienza University of Rome

Via Eudossiana, 18 - 00184 Rome, Italy

andrea.arcangeli89@gmail.com, carlo.bongioanni@uniroma1.it, nertjana.ustalli@uniroma1.it, debora.pastina@uniroma1.it, pierfrancesco.lombardo@uniroma1.it

Abstract—The focus of this paper is on the detection of airborne targets and on the estimation of their velocity by means of passive forward scatter radar systems based on the DVB-S as transmitter of opportunity. Results related to an experimental campaign carried out near “Leonardo Da Vinci” airport (Rome, Italy) are shown. Particularly the Doppler signature spectrogram is analyzed for a single node FSR configuration and time delay techniques are analyzed for a multi-static configuration suitable for velocity estimation. Obtained results clearly show the feasibility of the DVB-S based FSR configuration to reliably detect aircrafts and the effectiveness of the proposed velocity estimation techniques even in the near field area.

Keywords—forward scatter radar, transmitters of opportunity, motion estimation, spectrogram

I. INTRODUCTION

Forward Scatter Radar (FSR) systems are a particular configuration of bistatic radar where the bistatic angle is close to 180° , [1]. The main difference of the FSR system lies in its scattering nature. In the literature it is shown that the scattering signal in the forward direction is determined by the geometry, the motion parameters of the target and the size of the shadow contour, [1].

The FSR configuration presents several interesting advantages as the enhanced radar cross-section (RCS) compared to traditional radar geometries, a possibly long integration time due to little phase and amplitude fluctuation, robustness to the stealth technology. However there are some drawbacks in designing a system like this such as the absence of the range resolution and the operation within a narrow angle.

As the common bistatic radar, the FSR can operate with transmitters of opportunity dedicated to other purposes but found suitable for FSR operation such as DVB-T, GSM, DAB, FM etc. Specifically the potentialities of the passive FSR system for target detection in the far field area have been investigated in different works, [2]-[5].

Due to its almost total invulnerability to natural disasters, satellites as opportunity illuminators are of special interest. In particular Digital Video Broadcasting satellite (DVB-S)

provide a very wide coverage but the power density is very low. To improve target detection, the forward scattering concept may be investigated as an enhanced RCS in the forward direction is obtained. Therefore this work focuses on airborne target detection and motion parameter estimation by exploiting the DVB-S signal in a FSR configuration.

The paper is organized as follows. Firstly the geometry used throughout this work and the forward scatter signal model are briefly introduced in Section II. Experimental set-up and results of aircraft detection are shown in Section III while in Section IV the velocity estimation based (i) on the Doppler signature spectrogram of the single baseline and (ii) on the joint processing of the signals acquired by FSR system comprising two different receivers (Rx) are analyzed and compared. Conclusion closes the paper.

II. ACQUISITION GEOMETRY AND FS SIGNAL MODEL

The DVB-S based FSR system geometry is shown in Fig. 1. In our analysis, because geostationary satellites are used as emitters of opportunity, transmitter (Tx) has a fixed position specified in the ECEF coordinates system, and a long baseline L , in the order of the height of their orbit (35.786 km), is considered.

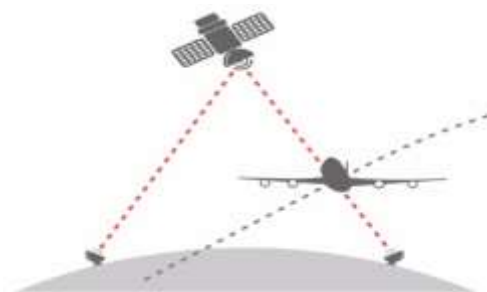


Fig. 1 - Passive FSR configuration based on the TV satellite broadcast.

With respect to the GPS based FSR configuration ([2], [5]), which is able to receive the signal anywhere on the Earth as almost four GPS satellites are continuously in view, in this case a precise positioning and pointing of the receiving antennas is required, aimed at (i) properly receiving the signal from the geostationary satellite and (ii) guaranteeing the

achievement of an actual forward configuration with the target intersecting the baseline while following its route.

In such FSR configuration, the received signal (in the absence of disturbance) is the sum of the direct signal from the transmitter and the scattered signal due to the presence of the target. Due to the target movement, the scattered signal presents a Doppler variation with an amplitude modulation specified by the FS pattern and by the propagation losses, [1]. Following the processing presented in [1], the received signal is passed through an envelope detector with quadrature characteristic which is followed by a decimation stage in order to reduce the sample rate and by the removal of the continuous component (DC).

Assuming that the target is following an almost linear trajectory, the resulting signal is a double-sided chirp signal, [1], and may be written as:

$$s_T(t) = \varepsilon(t) \sin \varphi_t(t) \quad (1)$$

where $\varepsilon(t)$ is the FS pattern and $\varphi_t(t)$ is the phase variation. In (1) we assume that the phase shift of the target signal, with respect to the direct signal, is defined by the path difference:

$$\varphi_t(t) = \frac{2\pi}{\lambda} [R_{Tx}(t) + R_{Rx}(t) - L] \quad (2)$$

where $R_{Tx}(t)$ and $R_{Rx}(t)$ are respectively the target-transmitter and target-receiver distances, that vary with times.

It is worth mentioning that in this scenario the target dimensions are much bigger than the signal wavelength so that we are operating in the optical scattering region and as a result an enhanced RCS is expected.

The target will be considered in the far field area of both the transmitter and the receiver if the far field parameter $S = 2l^2/\lambda R_{Tx}$ ($2l^2/\lambda R_{Rx}$) $\ll 1$, where l is the maximum dimension of the target, λ is the wavelength.

III. EXPERIMENTAL SET-UP AND DATA COLLECTION

In this section the acquisition campaigns set-up is described and the corresponding experimental results (in terms of target signatures) are reported.

A. Acquisition campaigns set-up

For the experimental campaign Hotbird 13D is the satellite selected from the geostationary satellites fleet HotBird 13°E, where European television broadcast entrusts their transmissions: the aim is to detect planes landing at “Leonardo Da Vinci” airport of Rome following the 16R runway.

By means of an accurate study of the International Approach Chart (IAC) provided by ICAO (see Fig. 2) the altitude of the aircraft, during the approach to the runway, is known. As the positions of the Tx and of the aircraft when landing on the 16R runway in the ECEF system are known, it is possible to determinate suitable positions of the receiving antenna as the intersections between the lines joining the transmitter and the different target positions and the ellipsoid representing the Earth (WGS-84).

The above procedure provides many alternatives for receiver location: some of them are shown in Fig. 3 where each position is labelled with the value of the altitude (h) of the aircraft when overlying that area being the red line the target trajectory. Among the positions provided, two of these were chosen named as North antenna ($h=435\text{ m}$) and South antenna ($h=437\text{ m}$) according to their position with respect to the North (Fig. 4).

Due to the particular geometry, with L in the order of 35.786 km, and due to the fact that we are looking for aircrafts landing at the airport, it is reasonable to approximate the distance target-Rx when the target crosses the baseline with the altitude of the aircraft overflying the receiver, $R_0 = h$.

In addition it is also possible to retrieve the value of baseline crossing angle since the nominal altitude of the aircraft during its approach to the runway is known, as previously mentioned. At a first approximation, after projecting the positions of Tx, Rx and aircraft (when approaching the 16R runway) onto a 2D coordinate system by dropping the altitude information, the baseline crossing angle is equal to $\theta = 64.2^\circ$.



Fig. 2 - 16R-Instrumental approach chart.

As previously mentioned, Hotbird 13D is the satellite chosen and among the TV channels available in the signal spectrum the RAI packet signal is exploited as signal of opportunity, with carrier frequency $f = 10.992\text{ GHz}$ ($\lambda = 2.73\text{ cm}$) and bandwidth $B = 37.125\text{ MHz}$.



Fig. 3 - Examples of suitable locations for the receiving antenna.



Fig. 4 - Location of the receiving antennas.

In this condition, it is clear that the target is always in the far field area of the Tx because of the long baseline, whereas in contrast, considering the distance target-Rx previously defined and the exploited short wavelength, aircraft targets with dimension in the order of 35-70 meters are in the near field of the receiver.

The fundamental components of the receiving chain used during the acquisition campaign are sketched in Fig. 5.

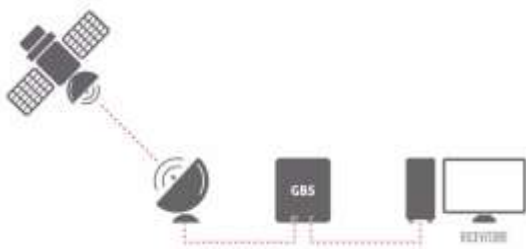


Fig. 5 - Receiving chain

Commercial parabolic antennas with 80 cm diameter were used, followed by an antenna amplifier (GBS) that substitutes the decoder. In fact the GBS role is to feed the local oscillator of Low Noise Block (LNB) located in the parabola focus. The satellite signals in the LNB are properly filtered and amplified by means of band-pass filter and low-noise-amplifier, respectively. Then, the carrier frequency is translated to an intermediate value of 1242 MHz. After these blocks the receiver is the same already described in [7].

In order to record navigation data of the aircrafts that cross the baseline and to guarantee the ground truth for the velocity estimation methods here considered, an ADS-B receiver was activated.

B. Experimental results

During the campaign all acquisitions were done with sampling frequency $F_s=25\text{MHz}$ that is the higher sample rate allowed by the receiver. Since the signal bandwidth is around 37 MHz this implies that the acquired signal is not the complete signal. Nevertheless, as the aim is not the reconstruction of the full signal but only of the modulation introduced by the crossing target, a sampling rate lower than the signal bandwidth does not influence the results.

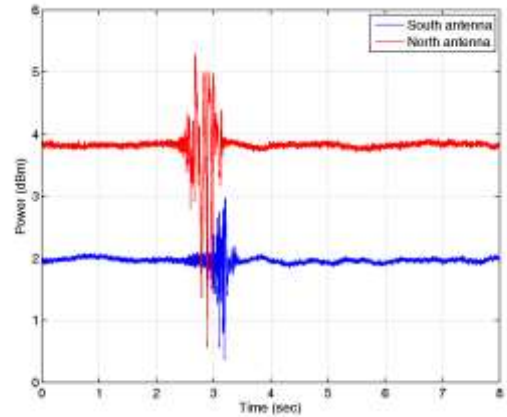


Fig. 6 - Time signature of the first dataset.

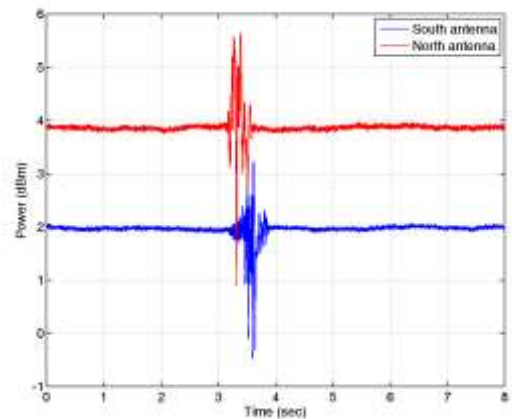


Fig. 7 - Time signature of the second dataset.

Following the processing described in section II, after the square law detector a decimation factor of 8^5 is performed, so that the acquired signal is down-sampled to $F_{s2}=763\text{Hz}$ suitable for the not ambiguous observation of the target Doppler signature.

Time domain signatures of different datasets collected from both antennas are shown in Fig. 6-Fig. 8. As it can be observed from Fig. 6-Fig. 8, the amplitude modulation due to the target crossing the baseline is noticeable. We also notice that there are acquisitions where the target signatures

recorded at the south and north antennas show appreciable differences: this behavior can be easily explained by considering that the FSCS depends on the shape of the target's silhouette and it may happen that the aircrafts did not cross the two baselines with the same part of the structures due to landing maneuvers.

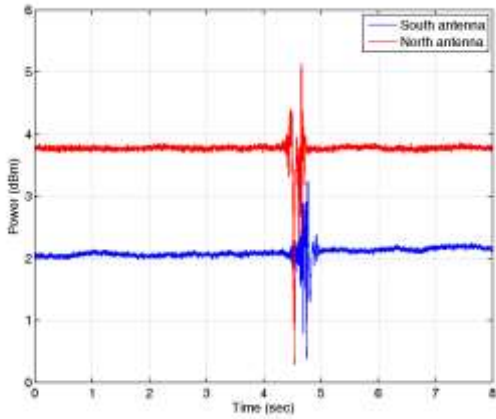


Fig. 8 - Time signature of the third dataset.

IV. VELOCITY ESTIMATION

In this section two approaches are considered for velocity estimation, based respectively on a single baseline configuration and on a two baseline configuration.

A. Single baseline configuration: Spectrogram analysis

The signal acquired by a single node FSR configuration is now analyzed for velocity estimation through a time-frequency analysis such as the Short Time Fourier Transform (STFT) which has been proven suitable for the extraction of the kinematic information for a target in the far field area, [6],[8].

Based in the assumption that the target follows a linear trajectory and by considering a Taylor expansion of the bistatic distance at the second order around the crossing time

instant, (see (2)) the Doppler rate as function of the motion parameters is expressed as follows:

$$f_d = \frac{1}{2\pi} \frac{d^2\varphi_t(t)}{dt^2} = \frac{(v \cos \theta)^2}{\lambda} \left(\frac{1}{L - R_0} + \frac{1}{R_0} \right) \quad (3)$$

where the parameters in (3) have been defined in the previous section; due to the very long baseline eq. (3) can be approximated as:

$$f_d \cong \frac{(v \cos \theta)^2}{\lambda} \frac{1}{R_0} \quad (4)$$

Fig. 8 (a) and Fig. 8 (b) show the spectrograms (each normalized with respect to its maximum value and reported in dB) of the signal received from respectively the North and the South antenna for the first dataset (Fig. 6). The duration of the target signature for both acquisitions is about 0.6 seconds and the dimension of the Hamming window for the estimation of the STFT is set equal to 0.16 sec. It is clear the correspondence between the spectrograms and the corresponding time signatures received from the North and the South antenna in terms of crossing point located respectively at 2.8 sec and 3.3 sec.

In accordance with the geometry introduced in section III, as the baseline crossing angle is $\theta \approx 64.2^\circ$ and the baseline crossing point may be approximated with the altitude of the aircraft when overlying each antenna, $R_0 \approx h = 435 \text{ m}$ for the South antenna and $R_0 \approx h = 437 \text{ m}$ for the North antenna, it is possible to estimate the velocity in agreement with (4). In Table I the estimated Doppler rate (as extracted from the slope of the target line in the spectrogram domain) and the estimated velocity are reported and an acceptable agreement with the velocity provided by the ADS-B can be observed.

Even though the target is in the near field area, from the spectrogram it is still possible to estimate the Doppler rate.

Moreover due to the exploited geometry, it is reasonable to consider the two baselines almost parallel and the same Doppler rate from both antennas is obtained.

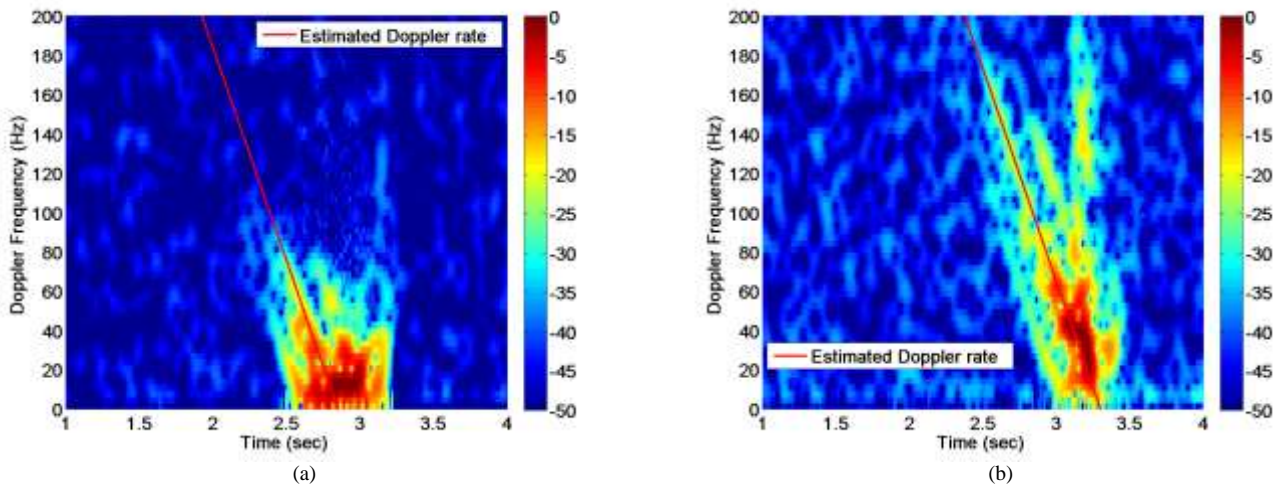


Fig. 9 - Spectrograms of the first dataset received (a) from the North antenna and (b) from the South antenna.

Table I Doppler rate and velocity estimated from the spectrograms

	f_d estimated (Hz/s)	v_{ADS-B} (m/s)	$v_{estimated}$ (m/s)	Error %
North Antenna	214	136.2	116	20.2
South Antenna	216	136.2	116.6	19.6

However, to estimate the target velocity, the above procedure requires a priori knowledge of two parameters, namely the crossing angle, θ , and the baseline crossing point, R_0 . In order to reduce this limitation a configuration based on two nodes is considered in the following sub-section.

B. Multi-static configuration: Time delay methods

The approaches here proposed are based solely on the exploitation of the time delay (namely the difference of the crossing instants) between the received signals at the two antennas and assume that the target is maintaining a constant velocity while crossing the two baselines.

Since the distance between the two antennas is $d=40$ m this assumption can be regarded reasonable. In addition, as mentioned previously, it is reasonable to consider the two baselines almost parallel and consequently the distance covered by the target between the two baselines can be assumed equal to the spacing between the two antennas, d .

Two methods are considered (Fig. 10): the first one, named “Start” method, estimates the beginning of the perturbation in the two received signals while the second one, “Bar” method, estimates the barycenter of the perturbation in the two signals.

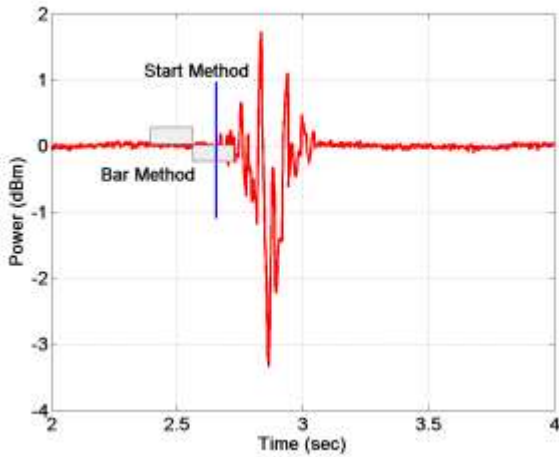


Fig. 10 - Speed estimation methods.

Table II reports the estimated velocity compared with the velocity obtained from the ADS-B for the three acquisitions which time signatures are reported in Fig. 6-Fig. 8.

From the table a good agreement between the estimated velocity and the velocity of the ADS-B is noted. Exploiting a multi-static configuration a reliable estimate of the velocity is obtained, particularly by the “Bar” method, without requiring the knowledge of other parameters as baseline crossing angle or baseline crossing point.

Table II Velocity estimation based on the time delay

	v_{ADS-B} (m/s)	“Start” (m/s)	Error %	“Bar” (m/s)	Error %
First dataset	136.2	88.7	31	123.1	9
Second dataset	151.8	200.8	32	146.7	3
Third dataset	156	158.9	2	173.4	11

V. CONCLUSION

In this work the feasibility of the DVB-S based FSR configuration for air target detection has been shown through different experimental results. Moreover some preliminary results concerning the estimation of speed of the target have been presented. Particularly two different approaches have been considered for velocity estimation, based respectively on a single baseline configuration and on a two baseline configuration. The results have shown that despite the near field condition it is still possible to estimate the Doppler rate from the spectrogram: such information combined with some a-priori knowledge (the baseline crossing angle and the baseline crossing point) allows to estimate the target velocity. Finally, a multi-static configuration comprising two baselines has been considered and crossing-times based strategies for velocity estimation have been presented. Obtained results prove that in this case a good estimate of the target speed can be obtained without requiring any a priori knowledge.

REFERENCES

- [1] M. Gashinova, L. Daniel, V. Sizov, E. Hoare and M. Cherniakov, "Phenomenology of Doppler forward scatter radar for surface targets observation," in *Radar, Sonar & Navigation, IET*, vol.7, no.4, pp.422-432, April 2013.
- [2] I. Suberviola, I. Mayordomo and J. Mendizabal, "Experimental Results of Air Target Detection With a GPS Forward-Scattering Radar," in *IEEE Geoscience and Remote Sensing Letters*, vol. 9, no. 1, pp. 47-51, Jan. 2012.
- [3] M. Gashinova, L. Daniel, E. Hoare, K. Kabakchiev, M. Cherniakov and V. Sizov, "Forward scatter radar mode for passive coherent location systems," *2013 International Conference on Radar*, Adelaide, SA, 2013, pp. 235-239.
- [4] P. Krysik, K. Kulpa and P. Samczyński, "GSM based passive receiver using forward scatter radar geometry," *2013 14th International Radar Symposium (IRS)*, Dresden, 2013, pp. 637-642.
- [5] C. Kabakchiev, I. Garvanov, V. Behar and H. Röhling, "The experimental study of possibility for radar target detection in FSR using L1-based non-cooperative transmitter," *2013 14th International Radar Symposium (IRS)*, Dresden, 2013, pp. 625-630.
- [6] M. Contu, A. De Luca, S. Hristov, L. Daniel, A. Stove, M. Gashinova, M. Cherniakov, D. Pastina, P. Lombardo, A. Baruzzi, D. Cristallini "Passive Multi-frequency Forward-Scatter Radar Measurements of Airborne Targets using Broadcasting Signals", *IEEE Transactions on Aerospace and Electronic Systems*, in print.
- [7] A. Macera, C. Bongioanni, F. Colone, P. Lombardo, "Receiver Architecture for Multi-Standard Based Passive Bistatic Radar", *2013 IEEE Radar Conference*, Ottawa, Ontario, Canada, April 29 – May 3, 2013.
- [8] A. De Luca, M. Contu, S. Hristov, L. Daniel, M. Gashinova and M. Cherniakov, "FSR velocity estimation using spectrogram," *2016 17th International Radar Symposium (IRS)*, Krakow, 2016, pp. 1-5.